ISSN: 0974-2115
www.jchps.com Journal of Chemical and Pharmaceutical Sciences

Luminomagnetic hydroxyapatite nanoparticles for biomedical applications

S. Karthi[1], G. Suresh Kumar[2], E.K. Girija[1]*
[1]Department of Physics, Periyar University, Salem 636 011, Tamil Nadu, India
[2]Department of Physics, K. S. Rangasamy College of Arts and Science (Autonomous), Tiruchengode 637 215, Tamil Nadu, India
***Corresponding author: E-Mail: girijaeaswaradas@gmail.com**

ABSTRACT

Luminomagnetic Eu^{3+}/Gd^{3+} co-substituted hydroxyapatite (EG-HA) nanoparticles have been synthesized by microwave irradiation method. The synthesized EG-HA nanoparticles exhibited red emission and paramagnetic behavior which indicate that it can be a potential candidate for biomedical applications such as magnetic resonance imaging (MRI), fluorescence imaging and drug/gene delivery.

KEY WORDS: Luminomagnetic, Hydroxyapatite, nanoparticles, bioimaging.

1. INTRODUCTION

Recently luminomagnetic nanomaterials are drawing considerable attention due to their simultaneous fluorescent and magnetic properties which makes them appropriate contrast agents for the important tasks in MRI, fluorescence imaging, controlled drug release and specific targeting (Gindy, 2009; Liong, 2008; Li, 2014). The combination of optical and magnetic properties in a single material can provide a high sensitive/resolved fluorescence imaging, as well as noninvasive and high spatial resolution magnetic resonance imaging. Several luminomagnetic nanomaterials such as gold, silica, polymer and quantum dots with magnetic oxide nanoparticles were developed in recent years (Kim, 2010; Ow, 2005; Li, 2009; Chen, 2010). However toxicity and removal issues due to leakage of constituent ions of the above mentioned luminomagnetic materials restrict their wide applications. Hence number of studies have been focused on developing biocompatible luminomagnetic materials (Aharoni, 2006; Xie, 2008).

Recently, hydroxyapatite [HA, $Ca_{10}(PO_4)_6(OH)_2$] nanoparticles is an emerging material in multimodal molecular imaging because of their excellent biocompatibility, bioactivity, biodegradability and convenience for surface modification. HA is considered as a good candidate for biomedical applications since it is the main inorganic component of biological hard tissues such as bone and teeth (Dorozhkin, 2010; Boanini, 2010). HA nanoparticles are good host materials for various cations and anions and hence it can be optically and magnetically functionalized through rare earth ion substitution. Recently, Ln^{3+} (Eu^{3+}/Gd^{3+} and Tb^{3+}/Gd^{3+}) ions dual-doped HA nanoparticles have been reported as novel multifunctional bioprobes for magnetic resonance and cell imaging applications (Feng, 2011; Liu, 2014). The aim of the present work is synthesis and characterizations of luminomagnetic Eu^{3+}/Gd^{3+} co-substituted HA (EG-HA) nanoparticles by facile microwave irradiation method.

2. EXPERIMENTAL PROCEDURE

EG-HA nanoparticles were synthesized by microwave irradiation method. Appropriate amount of $Ca(NO_3)_2.4H_2O$, $Eu(NO_3)_3.6H_2O$, $Gd(NO_3)_3.6H_2O$, Na_2HPO_4 and Cetyl trimethylammonium bromide (CTAB) were dissolved in distilled water so that the molar ratios of (Eu+Gd)/(Ca+Eu+Gd) = 5 mol% and (Ca+Eu+Gd)/P = 1.67. The mixture of Na_2HPO_4 and CTAB was added dropwise into the solution containing $Ca(NO_3)_2.4H_2O$, $Eu(NO_3)_3.6H_2O$ and $Gd(NO_3)_3.6H_2O$ and stirred for 1 h at room temperature while maintaining the pH above 12 using 1 M NaOH. The mixture was then put in a microwave oven (2.45 GHz, 600 W) and irradiated with microwave for 15 min. The obtained precipitate was washed several times using distilled water and ethanol and then dried by hot air oven for 24 h at 110 °C. Pure HA was also synthesized by the above mentioned method for comparison.

Powder X-ray diffraction (XRD) patterns of the synthesized samples were recorded in Rigaku MiniFlex II diffractometer in the 2θ range between 20° - 60° with CuK_α radiation (1.5406 Å). The morphology of the samples was inspected using a scanning electron microscope (Zeiss Ultra Plus). The photoluminescence emission spectra of the samples were recorded using a Horiba Jobin Yvon spectrofluorometer. The magnetic property of the samples was characterized using vibrating sample magnetometer (Lake Shore VSM 7410) at room temperature. The fluorescence images were taken using a Zeiss, LSM 710 laser confocal scanning microscope with the excitation wavelength 488 nm.

3. RESULTS AND DISCUSSION

Fig. 1 shows the powder XRD pattern of the as prepared samples. All the diffraction peaks observed for both the samples matched well with the standard data for HA (JCPDS No. 09–0432) which confirms the formation of a pure HA phase. The calculated lattice parameters for HA and EG-HA are a = 0.9372 nm, c = 0.6843 nm and a = 0.9426 nm, c = 0.6900 nm respectively, which are in good agreement with the standard data (JCPDS No. 09–0432). It was observed that the intensity of the diffraction peaks decreased and FWHM increased when Eu^{3+} and Gd^{3+} ions

are simultaneously incorporated into HA. The average crystallite size (D) of the samples was calculated using Debye Scherrer formula $D = 0.9\ \lambda/\beta\ \cos\theta$, where λ is the wavelength of incident X-ray, θ is the corresponding Bragg's diffraction angle and β is full width hall maxima of the (0 0 2) peak. The average crystallite size of the nanoparticles are found to be 46.77 nm and 45.27 nm respectively for HA and EG-HA. These effects may be due to inhibiting effect of Eu and Gd on the growth of HA crystallites.

The HA structure reveals the existence of two nonequivalent cationic sites called Ca (I) sites and Ca (II) sites. The Ca (I) site is of C_3 symmetry surrounded by nine oxygen ions and Ca (II) site is of C_s symmetry surrounded by six oxygen ions and one OH^- ions (Boanini, 2010). Eu^{3+} ions mostly replace the Ca^{2+} ions located at Ca (II) site, which is located near the OH^- lattice columns (Ternane, 1999). Similarly, for Er^{3+}, Sm^{3+} and Gd^{3+} ions, Ca (II) site is the preferred location (Get'man, 2010; Alshemary, 2015).

The substitution of Ln^{3+} (Eu^{3+} and Gd^{3+}) for the Ca^{2+} ions in Ca (II) sites needs a charge compensation mechanism which can be described as:

$$Ln^{3+} + O^{2-} \leftrightarrow Ca^{2+} + OH^-$$

$$2Ln^{3+} + \square\ (\text{Vacancy}) \rightarrow 3Ca^{2+}$$

In the first mechanism, charge compensation was achieved by the replacement OH^- ion in HA structure and the formation of interstitial O^{2-} ion resulting in a product $Ca_{10-(x+y)}Eu_xGd_y(PO_4)_6(OH)_{2-(x+y)}O_{(x+y)}$. In another mechanism, the charge imbalance associated with the substitutions of $2Ln^{3+}$ ions for the Ca^{2+} (I) site is compensated by the creation of a single Ca vacancy resulting in a product of formula $Ca_{10-3(x+Y)}Eu_{2x}\square_xGd_{2y}\square_y\ (PO_4)_6(OH)_2$.

SEM image of HA and EG-HA samples are given in Fig. 2. HA consists of more aggregated spherical nanoparticles. Whereas EG-HA particles are loosely agglomerated rod-like smaller sized particles. The PL emission spectrum with an excitation at 350 nm is shown in Fig. 3(a). Two strong luminescence peaks at 592 nm and 617 nm, and the one weak at 654 nm in Fig. 3(a) could be ascribed to $^5D_0 \rightarrow {}^7F_1$, $^5D_0 \rightarrow {}^7F_2$ and $^5D_0 \rightarrow {}^7F_3$ transitions of Eu energy levels, respectively. $^5D_0 \rightarrow {}^7F_1$ transition is related to Eu^{3+} substitution in Ca (I) while to $^5D_0 \rightarrow {}^7F_2$ transition is due to the substitution of Eu^{3+} in Ca (II). The result shows that the $^5D_0 \rightarrow {}^7F_2$ transition emission intensity is higher than that of $^5D_0 \rightarrow {}^7F_1$ transition intensity, which indicates that majority of Eu^{3+} ions are substituted at ca (II) sites (Ternane, 1999). Confocal microscope image of EG-HA is shown in Fig. 3(b) which exhibits red emission.

The magnetic property of HA and EG-HA nanoparticles was evaluated by field dependent magnetization measurements at room temperature (Fig. 4). From the nature of the curve it is clear that HA exhibits diamagnetic behavior, whereas EG-HA nanoparticles exhibit paramagnetic nature due to the presence of Gd^{3+} ion because it has seven unpaired electrons in the outer orbital. The magnetization of EG-HA nanoparticles is 0.870 memu/g, this leads to large effects on both longitudinal and transverse proton relaxation of Gd^{3+} ions even at low applied magnetic fields. EG-HA nanoparticles with paramagnetic property may be useful as MRI contrast agent.

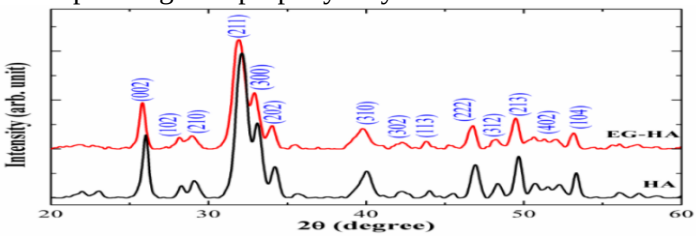

Fig.1.Powder XRD pattern of as prepared samples

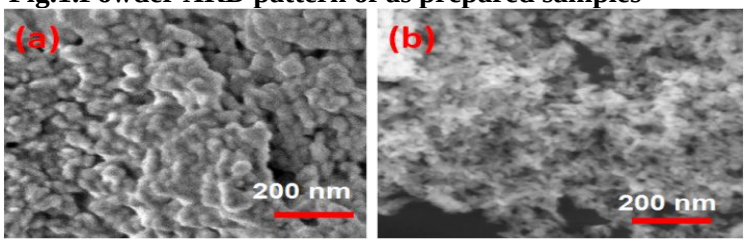

Fig.2.SEM images of (a) HA and (b) EG-HA nanoparticles

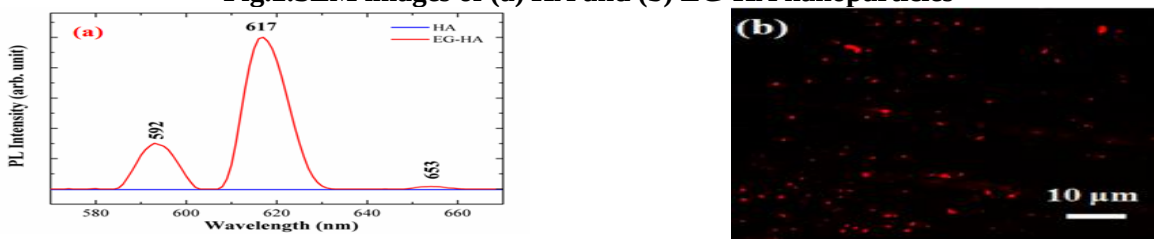

Fig.3(a)Photoluminescence emission spectra of the samples, (b) Confocal microscope image of EG-HA nanoparticles

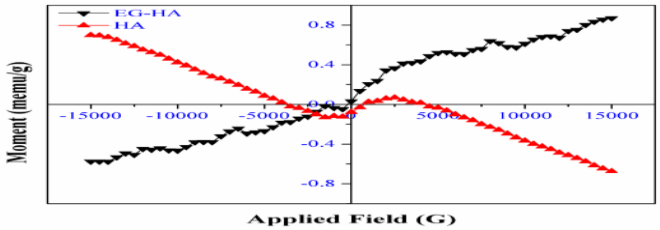

Fig.4.The magnetization curves of HA and EG-HA nanoparticles

4. CONCLUSION

Eu^{3+}/Gd^{3+} co-substituted HA nanoparticles were synthesized by microwave irradiation method. EG-HA nanoparticles exhibits both magnetic and luminescence properties. The present study offers a biocompatible luminomagnetic HA nanoparticle which can be used for diagnosis and therapy.

5. ACKNOWLEDGMENT

This work was financially supported by University Grants Commission, India through project (Project Ref. no. 41-1013/2012 SR).

REFERENCES

Aharoni A, Mokari T, Popov I, Banin U, Synthesis of InAs/CdSe/ZnSe core/shell1/shell2 structures with bright and stable near-infrared fluorescence, Journal of American Chemical Society, 128, 2006, 257-264.

Alshemary AZ, Structural characterization, optical properties and in vitro bioactivity of mesoporous erbium-doped hydroxyapatite, Journal of Alloys and Compouds, 645, 2015, 478-486.

Boanini E, Gazzano M, Bigi A, Ionic substitutions in calcium phosphates synthesized at low temperature, Acta Biomaterialia, 6, 2010, 1882 – 1894.

Chen FH, Synthesis of a novel magnetic drug delivery system composed of doxorubicin-conjugated Fe_3O_4 nanoparticle cores and a PEG-functionalized porous silica shell, Chemical Communication, 46, 2010, 8633−8635.

Dorozhkin SV, Nanosized and nanocrystalline calcium orthophosphates, Acta Biomaterialia, 6, 2010, 715 - 734.

Feng C, The photoluminescence, drug delivery and imaging properties of multifunctional Eu^{3+}/Gd^{3+} dual-doped hydroxyapatite nanorods, Biomaterials, 32, 2011, 9031- 9039.

Get'man EI, Isomorphous substitution of samarium and gadolinium for calcium hydroxyapatite structure, Russian Journal of Inorganic Chemistry, 55, 2010, 333-338.

Gindy ME, Prud'homme RK, Multifunctional nanoparticles for imaging, delivery and targeting in cancer therapy, Drug Delivery, 6, 2009, 865−878.

Kim D, Jeong YY, Jon S, A drug-loaded aptamer - gold nanoparticle bioconjugate for combined ct imaging and therapy of prostate cancer, ACS Nano, 4, 2010, 3689−3696.

Li Y, Chen T, Tan W, Talham DR, Synthesis of flower-like ZnO nanostructures by an organic-free hydrothermal process, Langmuir., 30, 2014, 5873−5879.

Li YL, Reversibly stabilized multifunctional dextran nanoparticles efficiently deliver doxorubicin into the nuclei of cancer cells, Angewandte Chemie International Edition, 48, 2009, 9914−9918.

Liong M, Multifunctional inorganic nanoparticles for imaging, targeting, and drug delivery, ACS Nano, 2, 2008, 889−896.

Liu, Synthesis and characterization of Tb^{3+}/Gd^{3+} dual-doped multifunctional hydroxyapatite nanoparticles, Ceramic International, 40, 2014, 2613 – 2617.

Ow H, Bright and stable core−shell fluorescent silica nanoparticles, Nano Letters, 5, 2005, 113−117.

Ternane R, Luminescent properties of Eu^{3+} in calcium hydroxyapatite, Journal of Luminescence, 81, 1999, 165-170.

Xie R, InAs/InP/ZnSe Core/Shell/Shell quantum dots as near-infrared emitters: bright, narrow- band, non-cadmium containing, and biocompatible, Nano Research, 1, 2008, 457-464.